Transparent stretchable capacitive touch sensor grid using ionic liquid electrodes

Ngoc Tan Nguyen, Mirza Sarwar, Claire Preston, Aziliz Le Goff, Cedric Plesse, Frederic Vidal, Eric Cattan, John D.W. Madden

Transparent stretchable capacitive touch sensor grid using ionic liquid electrodes

Ngoc Tan Nguyen [a,b,c], Mirza Saquib Sarwar [b], Claire Preston [b], Aziliz Le Goff [a,b], Cédric Plesse [d], Frédéric Vidal [d], Eric Cattan [a], John D.W. Madden [b,*]

[a] Univ. Polytechnique Hauts-de France, CNRS, Univ. Lille, Yncrea, Centrale Lille, UMR 8520 - IEMN, DOAE, F-59313 Valenciennes, France
[b] Advanced Materials and Process Engineering Laboratory, Electrical & Computer Engineering, University of British Columbia, Vancouver, BC, V6T 1Z4, Canada
[c] Department of Transportation Mechanical Engineering, The University of Danang - University of Science and Technology, 54, Nguyen Luong Bang, Danang, Viet Nam
[d] LPPI, EA2528, Institut des Matériaux, Université de Cergy-Pontoise, 5 mail Gay Lussac, Neuville sur Oise, F-95031 Cergy Cedex, France

Low cost soft, flexible and stretchable sensors are being explored that can be applied to virtually any surface, and promise to enable tactile sensing on robots, prosthetics, skin and stretchable displays. Previous work has shown that capacitive sensors that are both stretchable and transparent can be created by using ionically conductive hydrogel electrodes. In this study, the electrodes are interpen-etrating polymer networks swollen with ionic liquid, enabling high transparency and stretchability, without evaporation. The interpenetrating network is synthesized from poly(ethylene oxide) and nitrile butadiene rubber. Electrodes are patterned using femtosecond laser machining, creating stretchable electrodes. These were encapsulated in a polydimethylsiloxane substrate, producing a 95% transparent sensor (450 nm). A 4x4 tactile array shows the ability to sense proximity and multi-touch, as well as be robust to variations in environmental temperature (from 4 °C to 72 °C). Temperature change has a large effect on the resistance of the electrodes — an effect that could be used to measure device temperature. In addition, the sensor is able to detect proximity and touch while on skin, when covered by a layer of fabric or during stretch.

1. Introduction

Transparent and stretchable touch sensors have attracted attention as they could be used to provide sensory feedback in applications ranging from common handheld consumer electronics to advanced robotics and even prosthetics. These applications involve frequent human computer interactions combining touch overlaid on a visual display [1], stretch and/or bend and preferably stability in the face of changing temperature [2]. In addition, it may be useful to enable human machine interaction through a layer of material such as clothes. Two main approaches are capacitive and resistive sensing.

Various methods have been attempted to develop transparent and stretchable electrodes. They can be classified into three categories: geometric design of less stretchable materials, composite materials of conducting nanomaterials with stretchable elastomeric polymers, and the synthesis of intrinsically conducting polymers that are highly stretchable. In the first group, the stretchability of the electrodes can be achieved by patterning inorganic conductive materials like metals in a serpentine-like architecture [3–6], or depositing thin layers of silver nanowires (AgNW)s, carbon nanotubes (CNT)s or graphene [7,8] on elastomeric substrates that can be extended when the substrate underneath is stretched — or by pre-straining substrates [9]. A second route to obtain transparent and stretchable electrodes is the employment of nanocomposite materials such as AgNWs or CNTs mixed with elastomeric polymers such as PDMS or polyurethane-urea [10–12]. The third approach uses conducting polymers [13, 14] which are solution-process-able and pattern-able, to attain highly stretchable electrodes. In all these approaches, conductive materials must be kept very thin in order to maintain transparency. There is a challenge in combining soft stretchable materials and with stiff conductors. Even the conducting polymers are quite stiff and can only be stretched slowly. Nevertheless, devices fabricated using these stretchable conductor technologies have shown the ability to either detect touch [15–17], stretch [5, 6,10,18], bending [19], or all three — but without the ability to distinguish between them [20].

A fourth approach is to use ionic conductors. Ionic conductors can be both highly stretchable (by as much as 21x when tough

* Corresponding author.
E-mail address: jmadden@ece.ubc.ca (J.D.W. Madden).

hydrogels are employed) and extremely transparent (95%) [21]. The carriers – ions – have very low mobilities, and so are only suitable for applications involving small currents. Fortunately, capacitive sensors use only very low currents. These conductors are transparent because, unlike electrons and holes, they are so massive that they hardly move at visible light frequencies. They have been employed as stretchable electrodes in pressure sensors, electric-field driven actuators [20], and resistive touch sensors [22]. In our previous work [23], we demonstrated the use of a hydrogel electrode to perform proximity sensing, just as is done on most touch screens. A form of projected capacitance called mutual capacitance is used, in which field lines projected beyond the surface of the device couple with a finger or other approaching objects. The array detects a touch, and multi-touch, but is relatively insensitive to stretch and bend. A disadvantage of the approach is susceptibility to evaporation — which can be reduced by adding hygroscopic salts, but at the expense of conductivity [24] and, in turn, practical array size [23].

Building on this work, we demonstrate a mutual capacitance-based sensor that uses a semi-interpenetrating network (semi-IPN) polymer containing ionic liquid (IL) as electrodes. Advantages of this material combination include the ability to withstand high temperatures (180 °C in the case of ionic liquid used [25]), stretchability (140% [26]) and absence of evaporation. Among different types of semiIPNs, such as poly(ethylene oxide)/ hydroxytelechelic polybutadiene [27], poly(ethylene oxide)/ polytetrahydrofurane [28], poly(ethylene oxide)/ nitrile butadiene rubber (PEO/NBR) [29,30], NBR/PEO semiIPN shows quite good ionic conductivity (up to 0.13 S/m), high strain at break (150%) [31], and a small Young's modulus (330 kPa) [32]. In addition, the material shows good temperature stability. The ionic liquid incorporated into the semiIPN (1-Ethyl-3-methylimidazolium bis(trifluoromethanesulfonyl)imide: EMITFSI) has a decomposition temperature of 307 °C [23], while the semiIPN itself can be stable up to 180 °C [31]. These features, in addition to a high transparency, render the material suitable for a stretchable and transparent electrode.

In this paper we demonstrate transparency; proximity, touch and multi touch sensing with and without bending and stretching; and mechanical durability. The sensor array is designed to sense the approach and presence of a finger, which will cause a decrease in measured capacitance. Other grounded objects or objects with a large capacitance, such as other parts of the body or metal wires connected to ground, will also reduce capacitance as they approach. The array is relatively insensitive to pressure, stretch and bend. Novel aspects are the stability of its ionically conductive electrodes, which do not evaporate, and the investigation of temperature sensitivity of the measurement, showing how the use of lower frequency excitation can be used to eliminate temperature dependence, and how high frequency measurements might be used to measure temperature.

2. Fabrication

The fabrication of the sensor is based on a simple spin coating method. SemiIPN electrodes are first spin coated and the laser machined. Successive spin coating of dielectric elastomer layers that sandwich the two electrode layers creates the full structure.

2.1. Fabrication of semiIPN electrodes

The semiIPN is composed of a PEO ionically conductive phase, interpenetrated with elastomer NBR, which provides good elastic properties — with the resulting semiIPN being swollen with EMITSFI ionic liquid, which provides ion charge carriers. The EMITFSI, and the PEO are much more transparent in comparison to the NBR, which has a light yellow color. Here, since we expect a highly transparent stretchable semiIPN electrode, the ratio of NBR to PEO in the semiIPN structure was reduced relative to previous work on actuators [33] to minimize the yellowish color — while also maintaining the high stretchability.

The fabrication process of semiIPN described in [33] is briefly summarized as follow: the NBR solution (16 wt% NBR and 84 wt% cyclohexanone) was mixed with PEO precursors (75 wt% PEGM and 25 wt% PEGDM), where the ratio between the NBR and PEO is varied from 20% to 50%. A free radical initiator DCPD (3 wt% of PEO precursors) was then added to the mixture, stirred for 15 min, and degassed. A homogeneous mixture was obtained and spin-coated (600 rpm, 300 rpm s^{-1}, 30 s) on top of a silicon wafer. The polymerization was carried out under continuous supply of N_2 at 50 °C for 4 h to enable the formation of the PEO network.

The resulting semiIPN membrane was then swollen in EMITFSI for 3 days to allow it to reach the maximum swelling state. Finally, the sample was patterned by a femtosecond laser (Oxford Lasers, UV fundamental wavelength: 1064 nm, pulse length: 400 fs, spot size: 10 μm, galvanometric mirror resolution: 1 μm, maximum power 2 W) with patterning conditions of 10% power, 1 mm/s cutting speed, and 10 cut such that passes and electrodes were obtained.

2.2. Fabrication of sensor

The sensor fabrication process is mainly based on a highly reproducible precision coating technique combined with the fast femtosecond laser patterning method, as shown in Fig. 1a. In general, this fabrication includes three-step process where the first PDMS was spin-coated on a glass wafer following the first four semiIPN stripes containing disc electrodes. After the second PDMS dielectric layer was deposited, the second set of electrodes was laid down in a perpendicular direction to the previous set of electrodes. Finally, the third PDMS layer was deposited on these electrodes and spin-coated (details about the fabrication process can be found in S1).

Note that the spin coating method offers an easy means to tune the thickness of PDMS layer. The total thickness of the sensor was demonstrated to vary from approximately 300 μm to 1.5 mm by changing the spin coating speed. However, here we decided to conduct the characterization on a thick sensor (the total thickness: 550 ± 60 μm) as our readout circuit is restricted to values of capacitance < 4 pF.

2.3. Readout circuit

A capacitance to digital converter (CDC, AD7746) is used to measure the capacitance. The CDC estimates capacitance based on how much charge is transferred over 1/32,000th of a second. If the resistance of the circuit is significant – as in some of the measurements described below – the apparent capacitance is underestimated. In order to read the array, the signals are multiplexed (two MAX 4518, one each for the row and column electrodes). The output is directed to a microcontroller (ATmega 2560 8-bit). I2C protocol is used for the communication between the capacitance-to-digital-converters and the microcontroller and the data is read via a serial port. The marked rows and columns are described in Fig. 1b, and the complete system consists of the sensor and circuit is shown in Fig. 1c. The complete 4 x 4 matrix of 16 taxels is sampled at 3 Hz.

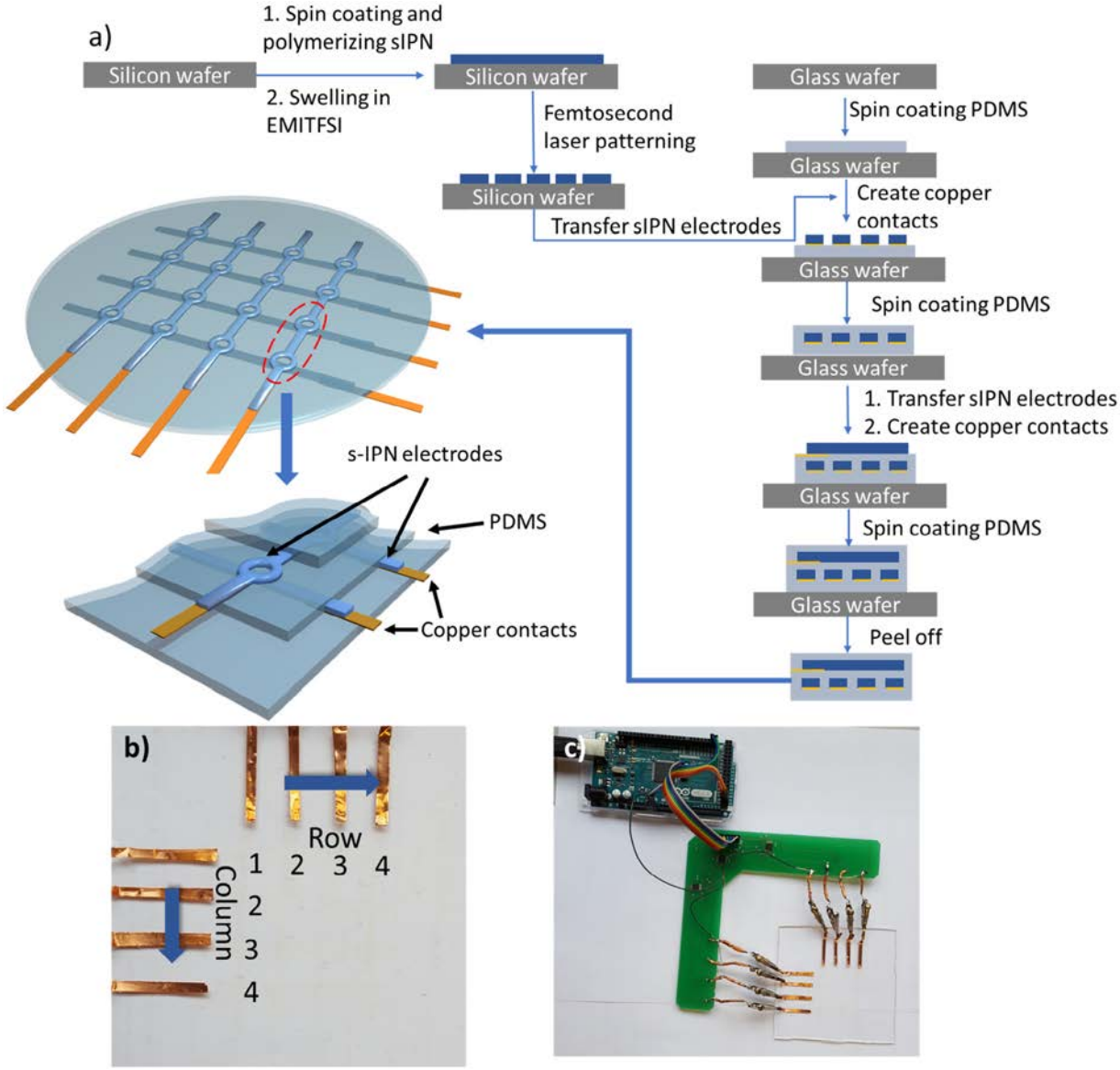

Fig. 1. (a) Layer by layer fabrication process of an artificial skin sensor and its structure, (b) Rows and columns of the electrodes, and (c) The sensor connected to the readout circuit.

3. Characterization

3.1. Transparency

An investigation on the transmittance through the fabricated sensor in the wavelength range of 400 nm–800 nm was performed using a Perkin-Elmer Lambda 800 UV–VIS spectrophotometer (semiIPN transparency optimization is described in S2.). As shown in Fig. 2a, the lowest optical transmittance here is 92% at a wavelength of 400 nm. In comparison to other PDMS based stretchable electrodes, such as silver nanowires/PDMS [34] and aligned CNT ribbon/PDMS [35] having a transmittance of 80%–90% and 60%, respectively, the 95% of transmittance at 450 nm meets the standards needed for high quality displays. There is nonetheless some quality loss due to the imperfectly flat surface of the material, as can be seen from the slight distortion of the inset image — where edges of the electrodes can be seen.

3.2. Temperature sensitivity

Temperature dependence of sensitivity complicates sensor readings since temperature needs to be known. Some recent work has investigated temperature sensing in stretchable arrays thanks to variation of metal resistance [36,37] under temperature changes. Here we explore the effect of temperature on our sensor response. When sampling at 32 kHz, there is a significant change in capacitance with temperature. We show that this can be eliminated by reducing the input measurement frequency to 10 kHz. As will be discussed, the reason that we see temperature effects on capacitance is because the resistance of the ionic liquid changes with temperature, which the capacitive sensing chip confuses with changes in capacitance. The change in ionic liquid resistance with temperature provides the ability to measure temperature, which may be desirable in prosthetic or robotic applications, for safety purposes for example, or to identify human touch. It may also be useful in medical sensor arrays.

In our stretchable transparent sensor, we instead use the conductivity variation of ionic liquid upon temperature change.

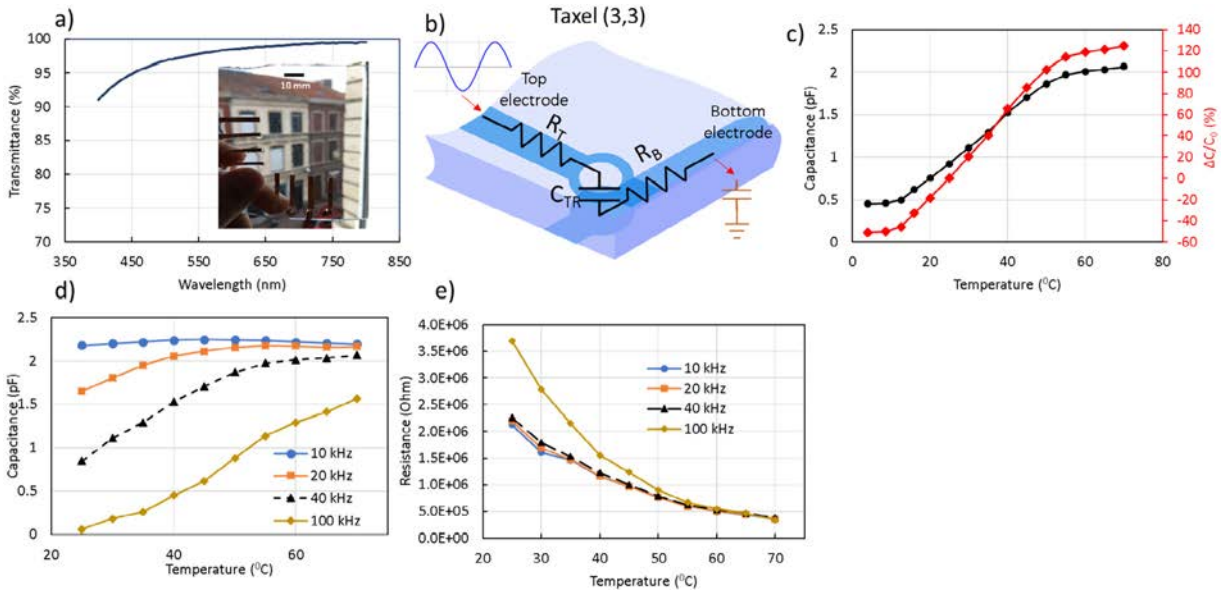

Fig. 2. (a) The optical transmittance versus wavelength plot for the resulting sensor with the 40%/60% ratio of NBR/PEO and the total thickness of 550 μm (the insert figure is a prototype of the artificial skin sensor), (b) An equivalent circuit model of taxel (3,) being measured, (c) Absolute capacitance value C_{TR} of the taxel (3, 3) (measured by circuit board) and relative capacitance (red) as a function of the temperature, (d) Temperature dependence of the absolute measured capacitance values (measured by multi-frequencies LCR meter) and (e) calculated resistances of taxel (3, 3) at sinusoidal excitation frequencies of 10 kHz, 20 kHz, 40 kHz, 100 kHz.

The first aim is to see whether exposure to temperature has an effect on the sensor readings once the sensor is returned to ambient conditions. The sensor was cooled to −4 °C using a refrigerator, and then heated to 100 °C using an oven, to see if exposure to a range of temperatures would change the response. Functionality was tested after the array returned to ambient temperature (23 °C). No change in behavior was seen.

In a second set of experiments, the capacitance evolution of the sensor was recorded while temperature changed from 4 °C to 72 °C (Fig. 2c). The capacitance of a taxel was measured (the 3,3 taxel near to the corner furthest from the connectors, where the effect of electrode resistance is large due to the long trace length). Between 8 °C to 55 °C, the capacitance value linearly increases from 0.5 pF to 1.99 pF at a rate of 3.4% / °C. It reaches a plateau when the temperature continues to increase up to 72 °C.

In the capacitance measuring chip, capacitance is estimated from charge accumulated in about 16 μs. If there is significant resistance in the circuit, represented by the resistances of the traces in Fig. 2b, this can slow the accumulation of charge, resulting in the underestimation of capacitance. Resistivity of ionic liquids is know to be a strong function of temperature [26,38], dropping as temperature increases. The increasing conductivity with temperature of semiIPN containing ionic liquids also shows a fast drop with increasing temperature [39]. Fig. 2c shows an apparent increase in capacitance of the sensor element with increasing temperature, which is consistent with the resistance hypothesis.

To further test this hypothesis, we measured capacitance and resistance over a range of frequencies. Considering the taxel (3,3), resistances of column 3 (top electrode), R_T, and row 3 (bottom electrode), R_B, respectively, as shown in Fig. 2b. Together with the coupling capacitance C_{TR} between the two electrodes, an $(R_T + R_B)C_{TR}$ time constant will be associated with this taxel. The data in Fig. 2d shows the measured capacitance value of taxel (3,3) as a function of temperature at frequencies of 10 kHz, 20 kHz, 40 kHz, and 100 kHz, obtained using an HP/AGILENT 4275A Multi-Frequency LCR Meter. When the excitation frequency is at 10 kHz, the capacitance remains constant as the temperature is varied from 25 °C to 70 °C. A stronger dependence of the capacitance on temperature is observed as the excitation frequency is increased. Fig. 2e shows that, as expected, the resistance drops as temperature increases. Practically, it also suggests that a low measurement frequency is appropriate for eliminating the temperature dependence of conductivity. The flat response at 10 kHz (Fig. 2d) suggests that resistance is no longer limiting estimation of the full capacitance. At this frequency, for the given values of resistance and capacitance, the sensor can operate effectively over a wide temperature range. The time constant, based on the resistance and capacitance estimate using the LCR meter measurement, is 6 μs, much shorter than the $1/(2\pi f) = 16\mu s$. The key to effective touch measurement is to measure at sufficiently low frequencies where the capacitance dominates the impedance [23]. Interestingly, by making measurements of impedance at high frequency, it should be possible to measure temperature.

3.3. Proximity, touch, and multi-touch sensing

In order to test proximity and touch response, the sensor is laid down on a flat surface and connected to the readout circuit. The sensor is able to detect the proximity when the finger moves within 2 cm of the surface, which is consistent with previous work on the same electrode geometry [23] and other work using a stretchable crossed grid of silver nanowire electrodes [40]. Fig. 3a shows the setup with a finger hovering above taxel (3, 3) at a distance of approximately 2 mm. The corresponding change in capacitance $\frac{\Delta C}{C_o}$ (where ΔC is the difference between the reduced capacitance due to the proximity and the steady state capacitance C_0) is plotted in the 3D bar plot in Fig. 3b, which shows a drop of 6%. It is observed that the position of the finger in plane can be easily interpreted from this data.

In the case of touching of a finger (Fig. 3c) a similar decrease in capacitance is observed but at higher magnitude (12%) as seen in Fig. 3d. Finger hover and contact with the surface are distinguished by the magnitude of drop in capacitance, as seen in Fig. 3e. This changing percentage capacitance is comparable to other stretchable capacitive touch sensors of similar electrode spacing that use thin gold films [41], silver nanowires [42], and silver nanowires/reduced graphene oxide [43] as electrodes,

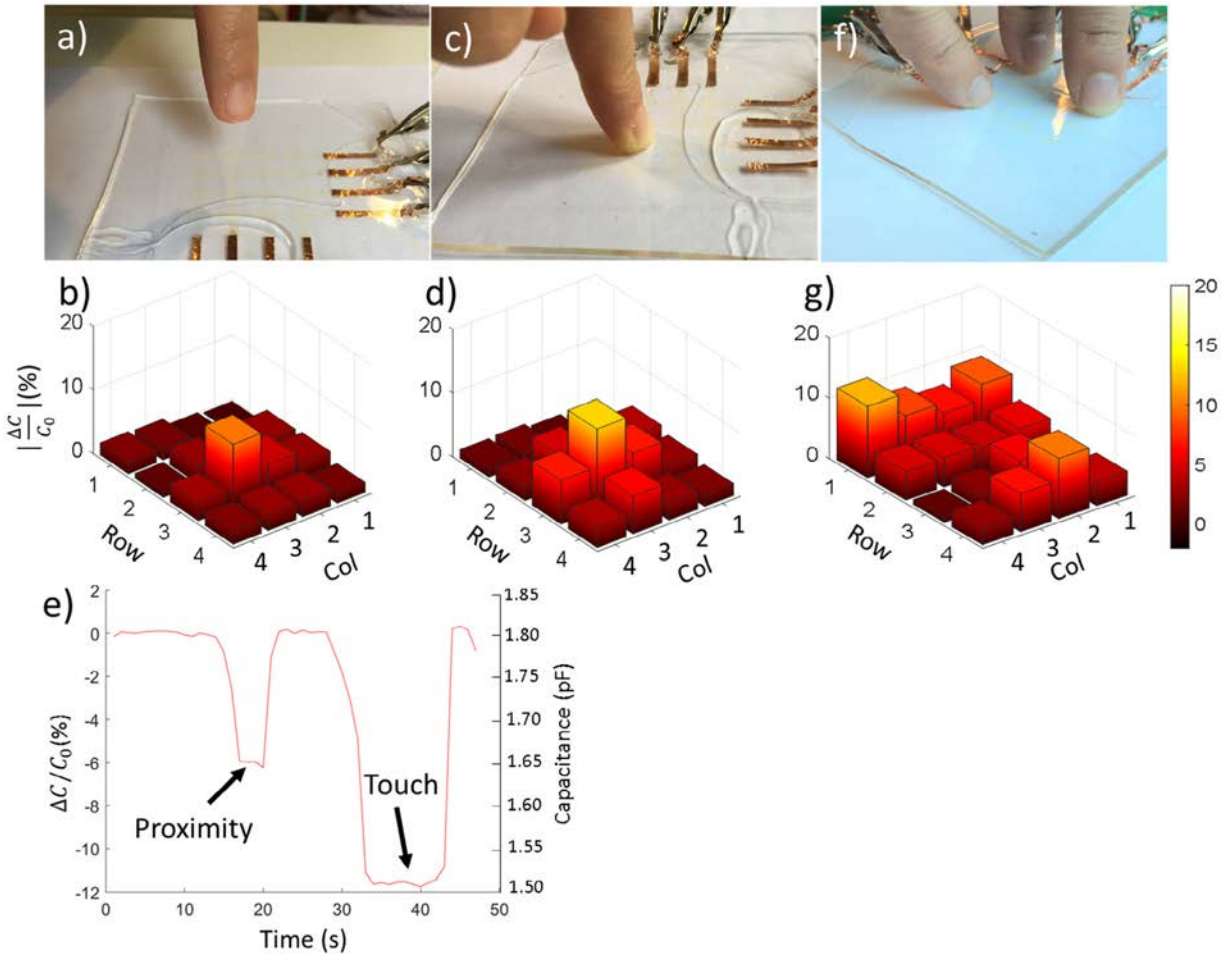

Fig. 3. (a) A proximity sensed while the finger approaches the sensor, and (b) the resulting decrease in capacitance of 8% due to this proximity. (c) Sensor being touched, and (d) the taxel touched showing a decrease in capacitance of 13%. (e) The capacitance value decreases upon proximity and touch, (f) Three fingers touch the sensor simultaneously, and (g) the change in capacitance with peaks showing the locations of touch.

where a finger touch induces a 25%, ∼18%, and 22% changing capacitance, respectively. These stretchable sensors are not transparent.

Similar to commercial touch screens, the sensor is able to recognize the multi-touch of the fingers (shown in Fig. 3f, g), where the locations of touch of three fingers are detected. The response time of the sensor is limited by the sampling rate of sensing circuit and the time to scan through the 4×4 matrix. Each taxel is sampled every 0.33 s. This sampling rate is slower than in a typical commercial touch screen, indicating that it should be possible to make this less than 10 ms by using less precise but faster electronics.

There is some cross-talk between adjacent taxels, as seen in Fig. 3d, which is expected given the proximity effects. One method of determining the center of touch is to compute the probability distribution, as is used in commercial device, leading to super-resolution — higher than that offered by the taxel spacing. The crosstalk may also be reduced by either (i) grounding all electrodes except the ones under test [44] instead of leaving them floating or (ii) adding another grounded conducting electrode underneath the sensor to reduce the effect of fringing field, but at the cost of losing proximity detection range.

3.4. Touch sensing while bending and stretching

Fig. 4a, b demonstrate the change in capacitance that results when the sensor array is folded. At a radius of curvature of approximately 3 mm, as shown in Fig. 4a, the induced strain on the electrodes is 3.7%, resulting in a maximum change in capacitance of 5% - similar to proximity signal, but lower than touch. Fig. 4c is a demonstration of the sensor's ability to detect a touch while being rolled. In this case the sensor is only rolled to a radius of curvature of 6 mm in order to avoid contact between two taxels or of the hand with the taxels while folding. Upon the bending, the capacitance values are decreased (< 4%) (Fig. 4b) due to interfering fringe fields. The sensor architecture, which contains pairs of loop and disc and thin top and bottom electrodes equally spaced to the neutral axis, ensures a high immunity from the bending effect [23]. A touch on the sensor while it is bent produces a peak with ∼15% decrease in capacitance value (Fig. 4d), making the touch clearly distinguishable from bending.

In Fig. 4e, f, the ability to detect a touch is demonstrated while the bottom half of the sensor is stretched. Fig. 4e shows the setup where the sensor is stretched by 30%, and is touched. A stretch excitation induces a linear decrease in capacitances of all the taxels in the bottom half by approximately 5% (Fig. 4f). The likely reason for this decrease is that the resistances of the electrodes being stretched are increased, resulting in a reduction of the apparent measured capacitances. At this stretched state, the sensor is still be able to detect a finger touch, inducing 12% of change in capacitance, as shown in Fig. 4f. An investigation on pressure sensitivity of the sensor is described in supplemental S3, showing that pressure results in a local increase in capacitance, and that this change is small for large applied forces (14 N) and stresses (100 kPa).

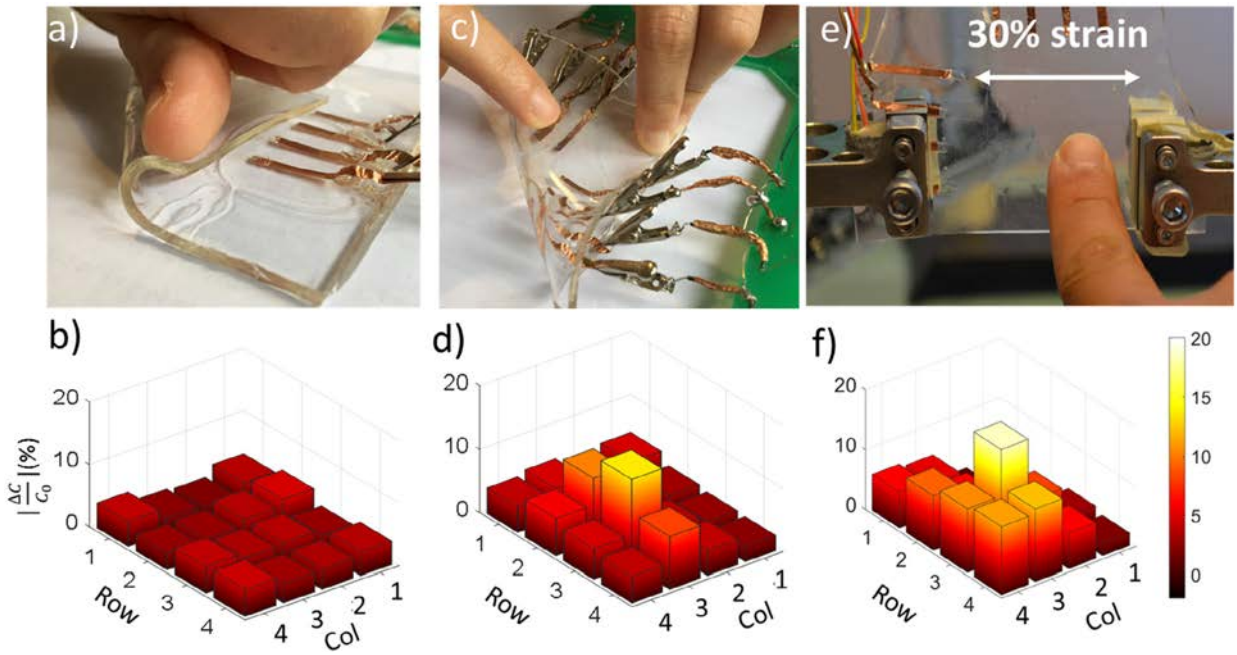

Fig. 4. (a) The sensor being folded, (b) Resulting a small change in capacitance value, (c) The sensor being touched while being bent, (d) A change in capacitance showing its ability to sense in bent state, (e) The sensor being stretched up to 30% strain and touched while stretched, and (f) The capacitances of the stretched taxels (columns 3 and 4) decrease, and the finger touch causes a further clearly visible decrease at 3, 3.

The effects of bending and stretch are small and more distributed in space than the effect of touch. This should make it possible to develop an algorithm that distinguishes touch from bend and stretch. Identifying proximity will be more challenging under conditions of active deformation, but may be possible based on the localization of the response.

3.5. Sensor applied on the skin and through fabric, and mechanical durability of the sensor

The sensor is composed mainly of PDMS, which has a low elastic modulus (360–870 kPa) [45], good biocompatibility, and high conformability to the skin. As shown in Fig. 5a, the sensor is being touched while placed on an arm. The arm acts as a large, grounded object, reducing all values of capacitance in the array by almost 20%. Fig. 5b demonstrates the sensor response upon touching while it is on the arm. In this case the base capacitance value, C_o, has been reset to the new background set by the presence of the skin. The touch is clearly visible.

For robotics applications involving interactions with humans, it may be desirable that the robots touch and 'feel' the presence of a human through clothing. Clothing has only a secondary effect on capacitance since it is not conductive and the dielectric constant is small. This sensor has the capability of detecting a touch through a layer of fabric, as shown in Fig. 5c, d. The corresponding change, $\frac{\Delta C}{C_0}$, is 10% upon contact between the finger and the two fabric layers made of 0.75 mm thick cotton (Fig. 5d). The fabric layer allows the fringe field to go through, however distances the finger from sensor surface. The penetrating field enables proximity and localization of the touch through cloth.

As an initial test of robustness against delamination, 500,000 tensile cycles at an amplitude of 10% were applied, showing no perceptible loss of sensitivity, as described in Supplement S4. The sensor array has also not changed in performance over the 30 months since it was initially fabricated, suggesting that the ionic liquid is being effectively contained.

The semiIPN itself can be stretched by more than 100% without any significant degradation [26]. Therefore, the stretchability of the sensor is limited only by the smaller elongation of the PDMS used here. The stretchability of the sensor can be further improved if the PDMS is replaced by other types of rubbers, such as Ecoflex®. The PDMS does have the advantage of high transparency [23].

4. Conclusion

A capacitive sensor, composed of ionic liquid swollen semiIPN, forming the electrodes, and PDMS dielectric layers, was fabricated using a simple process and low cost materials. The array can sense proximity and touch by a finger while placed on a flat surface, human skin, or when covered by layers of fabric. The effect of touch is clearly visible even when the sensor is bent or stretched. In addition, the sensor is transparent (95% at 450 nm), is resilient under repeated tensile strain, can withstand exposure to temperatures between −4 and 100 °C without loss of performance, and shows good shelf life. A sensitivity to temperature of 3.4%/°C was discovered, whose origin is the resistance change of the ionic liquid with temperature. This sensitivity is eliminated by measuring capacitance at a lower frequency, where capacitance dominates the impedance (10 kHz). The temperature dependence of resistance could be used in a temperature sensor.

Acknowledgments

This work was partly supported by the French Government through the National Research Agency (ANR) under program RENATECH, and by the Natural Sciences and Engineering Research Council of Canada (NSERC) through a Discovery Grant.

Appendix A. Supplementary data

Supplementary material related to this article can be found online at https://doi.org/10.1016/j.eml.2019.100574.

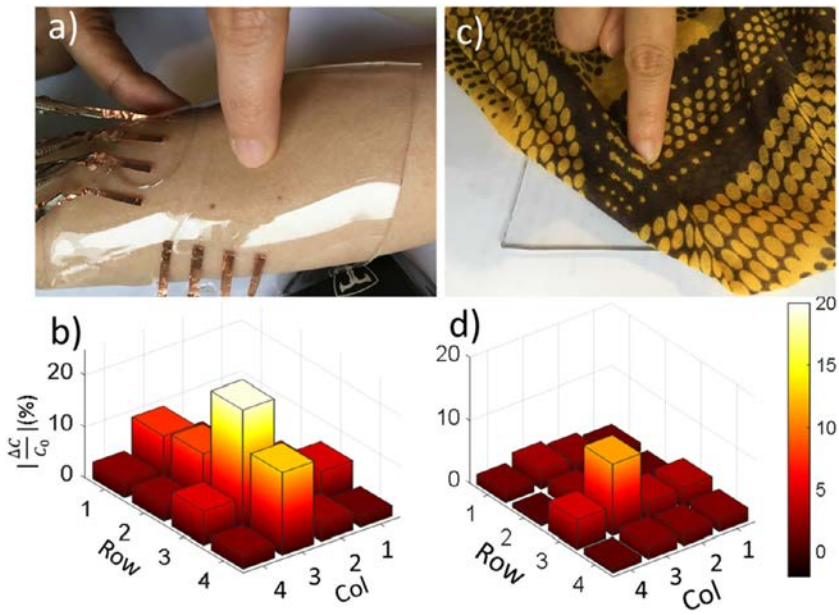

Fig. 5. (a) The sensor being touched while placed on the arm, and (b) the change in capacitance showing the ability to sense touch when on the arm. (c) and (d) Ability to sense the touch while being covered by fabric.

References

[1] J.H. Koo, D.C. Kim, H.J. Shim, T.-H. Kim, D.-H. Kim, Flexible and stretchable smart display: Materials, fabrication, device design, and system integration, Adv. Funct. Mater. 28 (35) (2018) 1801834.

[2] J. Kim, et al., Stretchable silicon nanoribbon electronics for skin prosthesis, Nature Commun. 5 (2014) 5747.

[3] R.H. Kim, et al., Stretchable, transparent graphene interconnects for arrays of microscale inorganic light emitting diodes on rubber substrates, Nano Lett. 11 (9) (2011) 3881–3886.

[4] S. Yang, E. Ng, N. Lu, Indium Tin Oxide (ITO) serpentine ribbons on soft substrates stretched beyond 100%, Extreme Mech. Lett. 2 (2015) 37–45.

[5] S. Han, et al., Fast plasmonic laser nanowelding for a Cu-nanowire percolation network for flexible transparent conductors and stretchable electronics, Adv. Mater. 26 (33) (2014) 5808–5814.

[6] K. Liu, et al., Carbon nanotube yarns with high tensile strength made by a twisting and shrinking method, Nanotechnology 21 (4) (2010) 045708.

[7] L. Cai, C. Wang, Carbon nanotube flexible and stretchable electronics, Nanoscale Res. Lett. 10 (1) (2015) 1013.

[8] F. Xu, X. Wang, Y. Zhu, Y. Zhu, Wavy ribbons of carbon nanotubes for stretchable conductors, Adv. Funct. Mater. 22 (6) (2012) 1279–1283.

[9] Y. Zhang, et al., Experimental and theoretical studies of serpentine microstructures bonded to prestrained elastomers for stretchable electronics, Adv. Funct. Mater. 24 (14) (2013) 2028–2037.

[10] D.J. Lipomi, et al., Skin-like pressure and strain sensors based on transparent elastic films of carbon nanotubes, Nature Nanotechnol. 6 (12) (2011) 788–792.

[11] T. Chen, H. Peng, M. Durstock, L. Dai, High-performance transparent and stretchable all-solid supercapacitors based on highly aligned carbon nanotube sheets, Sci. Rep. 4 (2014) 3612.

[12] J. Kim, J. Park, U. Jeong, J.-W. Park, Silver nanowire network embedded in polydimethylsiloxane as stretchable, transparent, and conductive substrates, J. Appl. Polym. Sci. 133 (33) (2016).

[13] M. Vosgueritchian, D.J. Lipomi, Z. Bao, Highly conductive and transparent PEDOT:PSS films with a fluorosurfactant for stretchable and flexible transparent electrodes, Adv. Funct. Mater. 22 (2) (2011) 421–428.

[14] P. Li, K. Sun, J. Ouyang, Stretchable and conductive polymer films prepared by solution blending, ACS Appl. Mater. Interfaces 7 (33) (2015) 18415–18423.

[15] T. Someya, T. Sekitani, S. Iba, Y. Kato, H. Kawaguchi, T. Sakurai, A. large area, Flexible pressure sensor matrix with organic field-effect transistors for artificial skin applications, Proc. Nat.l Acad. Sci. USA 101 (27) (2004) 9966–9970.

[16] W. Hu, X. Niu, R. Zhao, Q. Pei, Elastomeric transparent capacitive sensors based on an interpenetrating composite of silver nanowires and polyurethane, Appl. Phys. Lett. 102 (8) (2013) 083303.

[17] Mirza Saquib Sarwar, et al., Transparent and conformal 'piezoionic' touch sensor, in: SPIE Smart Structures and Materials Nondestructive Evaluation and Health Monitoring, 2015, 943026.

[18] C. Pang, et al., A flexible and highly sensitive strain-gauge sensor using reversible interlocking of nanofibres, Nat. Mater. 11 (9) (2012) 795–801.

[19] S. Park, et al., Stretchable energy-harvesting tactile electronic skin capable of differentiating multiple mechanical stimuli modes, Adv. Mater. 26 (43) (2014) 7324–7332.

[20] J.Y. Sun, C. Keplinger, G.M. Whitesides, Z. Suo, Ionic skin, Adv. Mater. 26 (45) (2014) 7608–7614.

[21] C. Keplinger, J.Y. Sun, C.C. Foo, P. Rothemund, G.M. Whitesides, Z. Suo, Stretchable, transparent, ionic conductors, Science 341 (6149) (2013) 984–987.

[22] C.C. Kim, H.H. Lee, K.H. Oh, J.Y. Sun, Highly stretchable, transparent ionic touch panel, Science 353 (6300) (2016) 682–687.

[23] M.S. Sarwar, Y. Dobashi, C. Preston, J.K. Wyss, S. Mirabbasi, J.D. Madden, Bend, stretch, and touch: Locating a finger on an actively deformed transparent sensor array, Sci. Adv. 3 (3) (2017) e1602200.

[24] P. Le Floch, et al., Wearable and washable conductors for active textiles, ACS Appl. Mater. Interfaces 9 (30) (2017) 25542–25552.

[25] L.J. Goujon, et al., Flexible solid polymer electrolytes based on nitrile butadiene rubber/poly(ethylene oxide) interpenetrating polymer networks containing either LiTFSI or EMITFSI, Macromolecules 44 (24) (2011) 9683–9691.

[26] D. Mecerreyes, Applications of Ionic Liquids in Polymer Science and Technology, Springer, Heidelberg, 2015, [Online]. Available.

[27] C. Plesse, F. Vidal, C. Gauthier, J.-M. Pelletier, C. Chevrot, D. Teyssié, Poly(ethylene oxide)/polybutadiene based IPNs synthesis and characterization, Polymer 48 (3) (2007) 696–703.

[28] C. Plesse, et al., Polyethylene oxide–polytetrahydrofurane–PEDOT conducting interpenetrating polymer networks for high speed actuators, Smart Mater. Struct. 20 (12) (2011) 124002.

[29] E. Marwanta, T. Mizumo, N. Nakamura, H. Ohno, Improved ionic conductivity of nitrile rubber/ionic liquid composites, Polymer 46 (11) (2005) 3795–3800.

[30] T. Ichino, M. Matsumoto, Y. Takeshita, J.S. Rutt, S. Nishi, New concept for polymer electrolyte: Dual-phase polymer electrolyte, Electrochim. Acta 40 (13) (1995) 2265–2268.

[31] F. Nicolas, M. Ali, P. Cédric, T. Dominique, C. Claude, V. Frédéric, Robust solid polymer electrolyte for conducting IPN actuators, Smart Mater. Struct. 22 (10) (2013) 104005.

[32] N. Ngoc Tan, et al., Nonlinear dynamic modeling of ultrathin conducting polymer actuators including inertial effects, Smart Mater. Struct. 27 (11) (2018) 115032.

[33] T.N. Nguyen, et al., Ultrathin electrochemically driven conducting polymer actuators: fabrication and electrochemomechanical characterization, Electrochim. Acta 265 (2018) 670–680.

[34] H. Weili, N. Xiaofan, L. Lu, Y. Sungryul, Y. Zhibin, P. Qibing, Intrinsically stretchable transparent electrodes based on silver-nanowire–crosslinked-polyacrylate composites, Nanotechnology 23 (34) (2012) 344002.

[35] Y. Zhang, et al., Polymer-embedded carbon nanotube ribbons for stretchable conductors, Adv. Mater. 22 (28) (2010) 3027–3031.
[36] N. Dossi, et al., An electrochemical gas sensor based on paper supported room temperature ionic liquids, Lab Chip 12 (1) (2012) 153–158, http://dx.doi.org/10.1039/C1LC20663J.
[37] A. Maziz, et al., Demonstrating kHz frequency actuation for conducting polymer microactuators, Adv. Funct. Mater. 24 (30) (2014) 4851–4859.
[38] Y. Cheng, R. Wang, H. Zhai, J. Sun, Stretchable electronic skin based on silver nanowire composite fiber electrodes for sensing pressure, proximity, and multidirectional strain, Nanoscale 9 (11) (2017) 3834–3842, http://dx.doi.org/10.1039/C7NR00121E.
[39] D.P.J. Cotton, I.M. Graz, S.P. Lacour, A multifunctional capacitive sensor for stretchable electronic skins, IEEE Sens. J. 9 (12) (2009) 2008–2009.
[40] S. Yao, Y. Zhu, Wearable multifunctional sensors using printed stretchable conductors made of silver nanowires, Nanoscale 6 (4) (2014) 2345–2352.
[41] T.Y. Choi, et al., Stretchable, transparent, and stretch-unresponsive capacitive touch sensor array with selectively patterned silver nanowires/reduced graphene oxide electrodes, ACS Appl. Mater. Interfaces 9 (21) (2017) 18022–18030.
[42] H.-C. Y., C.-L. C., P.-H. W., S.-J. Li, Elastic capacitive tactile array pressure sensor system, Sensors Mater. 29 (7) (2017) 10.
[43] D. Armani, C. Liu, N. Aluru, Re-configurable fluid circuits by PDMS elastomer micromachining, in: Technical Digest. IEEE International MEMS 99 Conference. Twelfth IEEE International Conference on Micro Electro Mechanical Systems (Cat. No.99CH36291), 1999, pp. 222–227.
[44] M.C. Belanger, Y. Marois, Hemocompatibility, biocompatibility, inflammatory and in vivo studies of primary reference materials low-density polyethylene and polydimethylsiloxane: a review, J. Biomed. Mater. Res. 58 (5) (2001) 467–477.
[45] A. Zahid, B. Dai, R. Hong, D. Zhang, Optical properties study of silicone polymer PDMS substrate surfaces modified by plasma treatment, Mater. Res. Exp. 4 (10) (2017) 105301.